

An Examination of the Radiation Sensitivity of Electronic Display Pixel Technologies

Landen D. Ryder¹, *Member, IEEE*, Edward J. Wyrwas², *Senior Member, IEEE*, Geraldo A. Cisneros³, Justin R. Bautista³, Xiaojing Xu⁴, Michael J. Campola¹, *Member, IEEE*, Razvan Gaza³, *Member, IEEE*,

¹NASA Goddard Space Flight Center, Greenbelt, MD 20771 USA

²SSAI Inc., Greenbelt, MD 20771 USA

³NASA Johnson Space Center, Houston, TX

⁴NASA Langley Research Center, Hampton, VA

Abstract—64 MeV proton irradiation were conducted on pixel technologies that spans the range of commercially available electronic displays for crewed missions. Human-centric optical performance metrics and at-facility characterization techniques are discussed and reported for assessment of pixel radiation susceptibilities.

Index Terms—Electronic Displays, Liquid Crystal Display (LCD), Light Emitting Diode (LED), Organic Light Emitting Diode (OLED), Electronic Ink/Paper (eInk), Thin-Film Transistor (TFT), Total Ionizing Dose (TID), Displacement Damage Dose (DDD)

I. INTRODUCTION

Recent commitments to return humans to the lunar surface and long duration crewed missions beyond the protection of the Earth's atmosphere and magnetosphere require examination of technologies and challenges that are unique to human inhabitants. Electronic displays serve as a critical, real time informational interchange between crew and the plethora of support technologies that contribute to a successful crewed mission (e.g., scientific instrumentation, safety and health monitors, computer interface, etc.). Critical components utilized in space-based applications must reliably operate through a variety of hostile environments such as the particle radiation environment comprised of galactic cosmic rays, trapped particle belts, and solar particle emissions. These highly energetic particles interact with materials at the atomic level, temporarily distorting free charge carrier populations and modifying intrinsic material parameters that in-turn impact the performance of devices built upon that material. Apollo Era spacecraft leveraged LEDs indicators and seven segment displays for relatively short duration lunar missions that inherently reduced the accumulated dose to the on-board displays [1]. Present-day utilization of electronic displays on the International Space Station and space tourism are confined to well-shielded spacecraft in low earth orbit altitudes with non-polar orbits which results in significantly attenuated energetic particle populations and radiation dose seen by on-board components [2]. In contrast, crewed missions to the lunar surface will subject electronic displays to a particle radiation environment without geomagnetic shielding and in some cases with little to no shielding at all (e.g., displays on an unpressurized lunar rover, surface-based instrumentation, etc.).

The maturation of the commercial electronic display market has resulted in a variety of mass-produced pixel technologies that can be integrated into systems ranging from small hand-held

biometric devices to large form-factor computer displays. The pixel technology is selected by system designers and manufacturers based on requirements such as cost, performance metrics, and resource constraints (size, weight, and power) rather than a need to use a distinct pixel technology. In this vein, the utilization of modernized commercial-of-the-shelf systems with electronic displays in lieu of custom manufactured system in crewed mission will require evaluation of the gambit of potential pixel technologies that is likely already integrated within a system. Given the realities of the small quantities required for space-based applications compared to the broader market, it is critical to evaluate potential design sensitivities while also understanding the tunable parameters (if any) within the electronic display fabrication and assembly process. In anticipation of extensive usage in future crewed missions, preemptive examination of radiation tolerance of commercially available electronic displays serves to reduce the risk volatility posed by the inclusion of electronic displays in upcoming crewed mission (NASA HEOMD-405 Integrated Exploration Capability Gaps List Tier 1 Gap 02-02).

To further develop the foundation of radiation effects in electronic displays, a 64 MeV proton irradiation test campaign was conducted to 1) develop the characterization and analysis techniques for electronic displays and 2) collect preliminary test data for broadly assessing the susceptibility of electronic display pixel technologies. Assessment of radiation-induced degradation in electronic displays requires the implementation of human-centric measurements (e.g., luminosity and chromaticity) within the constraints of traditional ground-based test facilities. From these test results, radiation-induced degradation in the pixel technology of organic light emitting diodes (OLEDs), backlight thin-film transistor liquid crystal displays (TFT-LCDs), and light emitting diode (LED) dot arrays was demonstrated and used to examine the significance of the red, green, and blue pixels degrading at distinct rates (non-uniform). The intent of this manuscript is to socialize the necessity of radiation tolerant electronic displays for future crewed missions, outline characterization and analysis techniques utilized for characterizing radiation-induced degradation in human-interface applications, and report test results from a cross-section of commercially available display technologies to grow the body-of-knowledge of commercially available electronic displays, in anticipation of the growing need for reliable electronic displays in a variety of radiation environments [3]-[4].

Pixel Technology	Pixel Drive Technique	Device Label	Screen During Irradiation	Dimensions	Part Number
LCD	Side Coupled LED with TFT BackPlane	LCD-1	Black	43mm x 60mm	Product ID: 2478
	Side Coupled LED with TFT BackPlane	LCD-2	White	43mm x 60mm	Product ID: 2478
	Side Coupled LED with TFT BackPlane	LCD-3	Black	43mm x 60mm	Product ID: 2478
	Side Coupled LED with TFT BackPlane	LCD-4	White	43mm x 60mm	Product ID: 2478
	Side Coupled LED with TFT BackPlane	LCD-5	White	56mm x 85mm	Product ID: 2050
OLED	Passive Matrix	OLED-1	Black	27mm x 27mm	Product ID: 1431
	Passive Matrix	OLED-2	Pins Grounded	27mm x 27mm	Product ID: 1431
	Passive Matrix	OLED-3	Black	27mm x 27mm	Product ID: 1431
	Passive Matrix	OLED-4	White	27mm x 27mm	Product ID: 1431
White LED Matrix	Conductive Array	WLED-1	Pins Grounded	20mm x 20mm	KWM-20882XWB
	Conductive Array	WLED-2	Pins Grounded	20mm x 20mm	KWM-20882XWB
	Conductive Array	WLED-3	Pins Grounded	20mm x 20mm	KWM-20882XWB
Blue LED Matrix	Conductive Array	BLED-1	Pins Grounded	30mm x 30mm	KWM-30881CBB
Monochrome E-Ink	Active Matrix	MEINK-1	Pins Grounded	28mm x 28mm	Product ID: 4196
Tricolor E-Ink	Active Matrix	TEINK-1	Pins Grounded	28mm x 28mm	Product ID: 4868

Table 1. Electronic displays that were irradiated in this test campaign Note that the dimensions correspond to the size of the display board which is slightly larger than the optical emission area of the screen.

II. DEVICE UNDER TEST

To best represent a cross-section of commercially available pixel technologies radiation data was collected on LCDs, OLEDs, LED matrices, and electronic ink/paper (eInk) electronic display screens (summarized in Table 1). Electronic display screens are comprised of tightly integrated functional layers that utilize a variety of material systems (e.g., polymers, glasses, light emission layers, optically transparent conductors) to enable proper, reliable operation; a notional diagram of an LCD screen with a backlight is provided in Fig. 1. It should be noted that in addition to actively modulated layers like light emission layers and conductive backplanes, there is a significant number of passive layers that provide structural support, environmental passivation, and optical filtering. Based on this functional decomposition, radiation susceptibility is expected to occur as 1) reduction in photon production efficiency of the light emission layers, 2) degradation of the electrical modulation technologies (e.g., shift in transistor threshold voltage), and 3) introduction of color centers in any layer that emitted photons must pass through [5]-[7].

The LCDs used in this test campaign utilize a thin-film transistor backplane to individually address pixels within the screen (also referred to as active matrix) to represent the architecture that most commercial LCD screens are built upon [8],[9]. Due to the small form factor of the display, light emitted from the electronic display originates from white LEDs positioned at one edge of the display and utilizes a “waveguide” material to distribute the light through the display (known as edge coupled) rather than the more common backlight configuration. For this display configuration, the light emission from a pixel is modulated via voltage controlled liquid crystal layers that polarize light passing through the layer and are filtered by a polarization filter. The benefit of this edge-couple configuration is that it removes light emission layer degradation as a potential contributor to any observed radiation-induced degradation and narrows the potential degradation mechanisms in the pixel to the plastic overburden (e.g., filters, polarizers, stabilizers), thin-film transistors, and the liquid crystals.

At the pixel level, the OLED display screen consists of an OLED, and associated color filter, with the anode and cathode connected to a grid of vertical and horizontal conductors that allows electrical modulation of light emission via the voltages applied along the conductors (also referred to as passive matrix)

[10]. The light emission and modulation layers are between two layers of glass to provide structural support and passivation. Based on layout of this passive matrix OLED display screen, any radiation-induced degradation can be localized to the light emission layer and the glass overlayer (row/column drivers located outside of the irradiated region).

The LED matrices examined in this test campaign utilize an array of InGaN LEDs on a conductive mesh with the final color of the LED determined by a phosphor coating. Two LED colors (blue and white) were used to provide two different LED spectra for examination [11],[12]. The lack of passive material stack-up or an active electronic modulation allows for isolation of degradation mechanism to the light emission region (well explored in literature) and provide a single emitter white light “display” as a point of comparison for the displays that utilize additive color mixing with colored pixels.

Though they are not typically used in a sub-second refresh rate like typical electronic displays, the final pixel technology that was examined in this test campaign were monochrome and tri-color eInk displays [13],[14]. These reflective displays function by the alignment of charged pigments via an electric field induced via a conductive mesh. As the charged pigment alignment will persist without an applied electric field, eInks find use in low power applications that require infrequent modification of displayed image. Based on the configuration of these eInk displays, the primary region of sensitivities would be confined to the charged pigments and the glass overlayers.

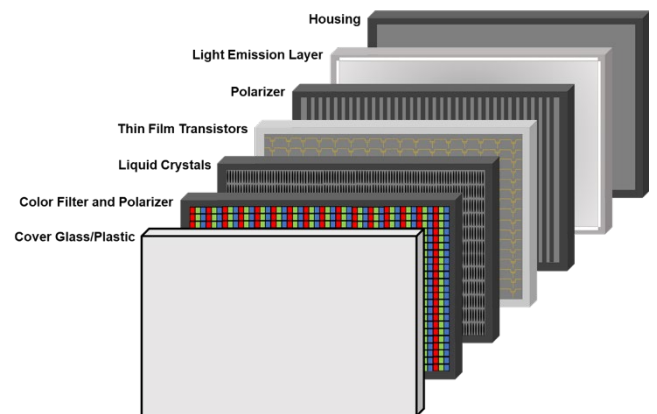


Fig. 1. Notional stack up of an LCD screen. Note that many of these functional layers will still be present in alternative pixel screen technologies.

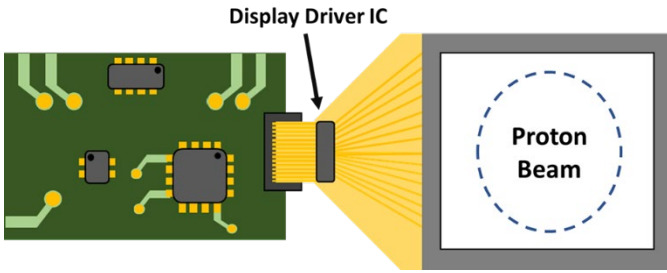


Fig. 2. Notional schematic of display boards and the modifications used in this measurement campaign. The screen containing the individual pixels are attached to an electronic board and display driver IC with a flexible tape connector. This allows for “unfolding” the display to center the beam on the screen and avoid support electronics.

III. TESTING APPROACH

This irradiation campaign focused on the use of small form factor, commercially available electronic displays that could be controlled with external microcontrollers with housing that could be easily modified for testing. As the intent of this test campaign is to probe the susceptibility of pixel technologies rather than the radiation hardness of any support circuitry, the tape connectors used to connect the pixel screen to the control circuitry can be unfurled to remove any sensitive support electronics from behind the screen (Fig. 2). Furthermore, beam apertures with spatial extent less than the area of the screen were used to confine the proton beam to ensure that only the pixel screen is being irradiated (apertures on the order of 1-inch diameters).

Proton irradiation was performed with 64 MeV protons at Crocker Nuclear at the University of California – Davis at ambient temperatures. SRIM calculations were used in conjunction with approximate dimensions to ensure that the overlayers did not significantly attenuate the proton energies reaching the regions of interest for the pixels [15]. The potential sensitivities to both total ionizing dose and displacement damage dose encouraged the use of this proton energy to investigate both degradation mechanisms simultaneously. For the purposes of this work displacement damage is reported as the fluence of 64 MeV protons; this allows for direct computation of displacement damage dose or to alternative equivalent particle fluences via NIEL scaling [16].

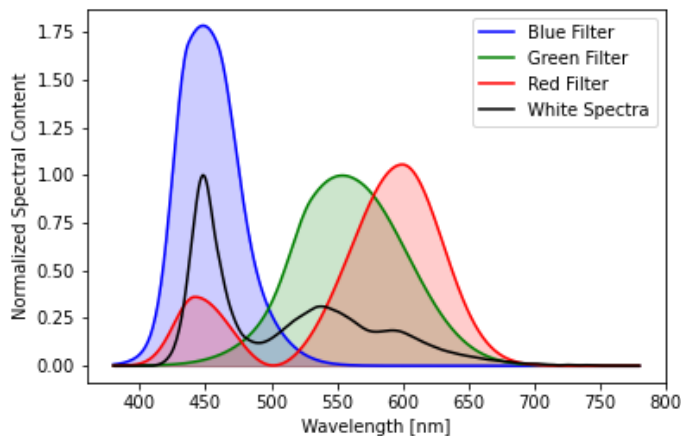


Fig. 3. The spectral response of the three categories of photoreceptive cones responsible for the visual perception of color and used to produce the tristimulus values used in color theory. An example white light spectra is provided to better visualize the wavelength spectra associated with each color.

Testing was performed in air at ambient room temperature with no additional cooling. Given the small size and lack of any intensive on board processing the electronic displays remain cool to the touch. During irradiation the electronic displays were driven with a microcontroller to output a monotone color (either black or white). The microcontroller was located away from the irradiated boards and display to ensure there was no adverse behavior related to secondary particles; no erroneous behavior consistent with complications from the microcontroller were observed during the test campaign. Following irradiation, electronic displays were removed from the beam line and placed in a custom “light box” that maintained consistent placement of the electronic displays relative to the Sekonic c7000 handheld spectrometer used in capturing optical spectra from the electronic displays. Electronic displays were driven to output a monotone color of red, blue, green, and white during optical characterization.

IV. ANALYSIS APPROACH

Given that performance criteria for electronic displays are evaluated from a human-user perspective, it is instructive to form the connection between traditional characterization metrics of microelectronics and optoelectronic devices and the metrics that are outlined in this report. LEDs find extensive use in unmanned spacecrafts (e.g., camera illumination, optoisolators, etc.) with radiation-induced degradation typically summarized as reduced output optical power and impact on the spectral content of the emitted light [17]. While this type of degradation will certainly be present the light emission regions of an electronic display, human-based applications necessitate that degradation be evaluated through the lens of visual perception due to the non-uniform spectral sensitivity of the human eye. Utilizing color theory, spectral measurements over the visible light wavelength range (380 nm to 780 nm) commonly captured during characterization of optoelectronics can be converted to common electronic display performance metrics and can be readily reproduced for post-irradiation assessment.

Functionally, electronic displays are intended to transmit to humans via the emission of photons that are in-turn transduced via photoreceptors (rods and cones) in the retina into visual characteristics such as “brightness” and color. These photoreceptive cones are divided into the three categories based upon spectral photosensitivity and create the visual perception

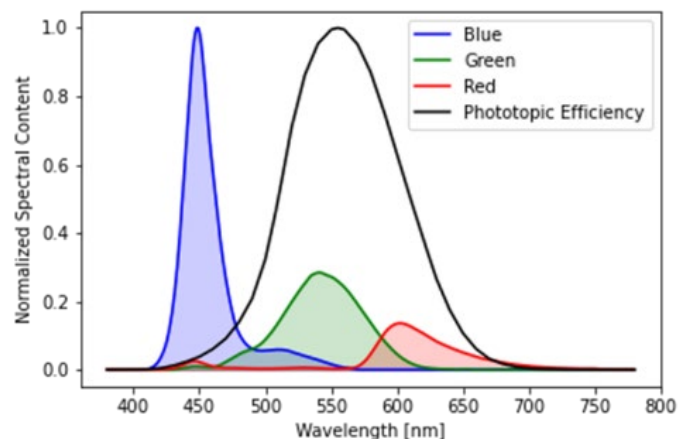


Fig. 4. The spectral content of a red, green, and blue pixel and the photopic efficiency function that is used for this analysis. Note the significant spectral overlap of efficiency function of the green and red pixels and much smaller overlap with the blue pixel.

Device Label	100 krad(Si) Dose	Maximum Test Dose - White Screen			RGB Color Shift - 24 bit Color		
	Luminous Intensity Normalized to PreRad Calues	64 MeV Proton Fluence [p ⁺ /cm ²]	Total Ionizing Dose	Luminous Intensity Normalized to PreRad Calues	Red	Green	Blue
LCD-1	86.50%	3.01E+12	175 krad(Si)	84.30%	0x07	0x08	0x0D
LCD-2	86.70%	2.58E+12	150 krad(Si)	83.10%	0x05	0x05	0x08
LCD-3	Driver IC inoperable after accidental irradiation	3.44E+11	20 krad(Si)	Driver IC inoperable after accidental irradiation	0x02	0x03	0x04
LCD-4		5.16E+11	30 krad(Si)		0x05	0x06	0x0A
LCD-5	90.00%	1.72E+12	100 krad(Si)	90.00%	0x04	0x04	0x07
OLED-1	89.80%	3.44E+12	200 krad(Si)	85.60%	0x06	0x01	0x06
OLED-2	83.60%	1.72E+12	100 krad(Si)	83.60%	0x01	0x01	0x01
OLED-3	93.20%	2.15E+12	125 krad(Si)	92.80%	0x05	0x01	0x03
OLED-4	92.50%	1.72E+12	100 krad(Si)	92.50%	0x04	0x00	0x03
WLED-1	87.70%	1.72E+12	100 krad(Si)	87.70%	0x01	0x00	0x01
WLED-2	82.50%			0x02	0x00	0x00	
WLED-3	91.90%			0x01	0x00	0x01	
BLED-1	83.80%	5.15E+12	300 krad(Si)	65.30%	0x00	0x01	0x00
MEINK-1	No visual degradation observed	1.72E+12	200 krad(Si)	No visual degradation observed			
TEINK-1	No visual degradation observed	1.72E+12	200 krad(Si)	No visual degradation observed			

Table 2. Summary of the results collected during this test campaign. Note that the 100 krad(Si) column is intended to allow for comparison of pixel technologies at a common dose point but is not the highest dose that a device was taken to.

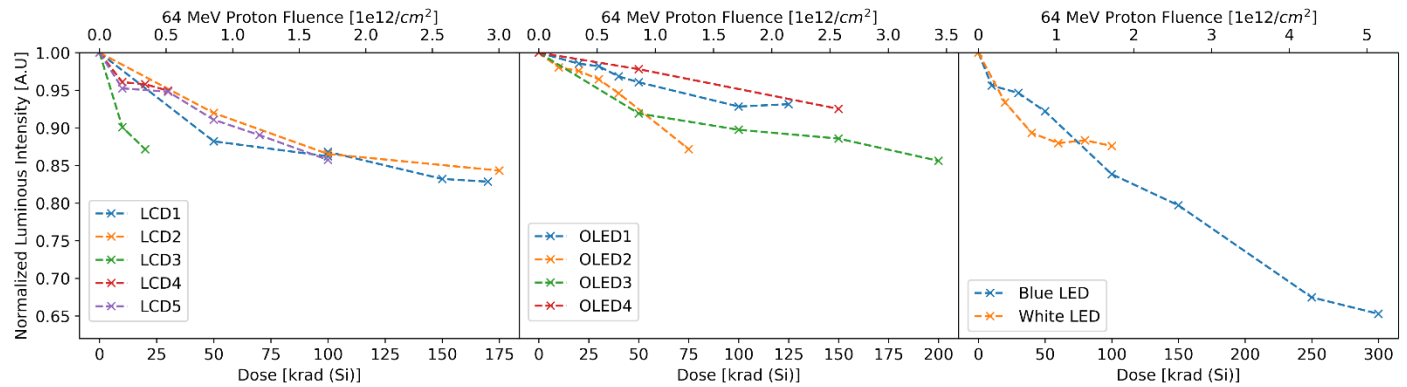


Fig. 5. Luminous intensity as a function of total ionizing dose/proton fluence normalized to pre-irradiation values for each emissive display examined in this test campaign. The low dose numbers for LCD3 and LCD4 were due to early failure from inadvertent exposures of the display drivers on the tape connector.

of color via an aggregation of neural responses for all three categories. Quantitative color theory is built upon the decomposition of visible light into three tristimulus parameters that are used to uniquely identify a color within a color space through the use of color matching function as spectral weights (provided in Fig. 3 for reference) [18]. From the perspective of radiation-induced degradation, these color matching functions allow for 1) optical spectra to quantify the color shift from nominal operation that a human would perceive as a function of dose and 2) better localization of the degradation mechanism within the pixel (e.g. degradation of blue pixels would result in a white screen appear with a shade of yellow).

While tristimulus values can be used to define a color space that visualize the color of a light source, there is an amount of obfuscation associated with quantifying color shift without the aid of a color space diagram. To combat this, tristimulus values were converted to the familiar sRGB color space commonly used in electronic display color mixing [19]. This allows for the measured color shift to be quantified as a bit shift in each channel of a n-bit color space. It should be noted that increasing the bit resolution of the color space will in-turn increase the size of the reported bit shift.

Similar to color mixing, the “brightness” of a light source relies on a luminosity function (representing the spectral sensitivity of the average human eye) as spectral “weight” to covert radial spectral flux (energy on a surface) of a conventional optical spectrum to something more akin to visual energy. The luminosity function used for the analysis in this work in addition to a blue, green, and red screen from an electronic display, is provided in Fig. 4 to demonstrate that red

and green pixels dominate the overall luminosity intensity of an electronic display. The analysis within this report utilizes the photopic luminosity function to collapse an optical spectrum from an electronic display into luminous quantities, but it should be noted that there alternative luminosity functions that could be useful for more tailored applications [20]. Mesoscopic (twilight) and scotopic (low light) luminosity functions can be used to define light constrained environments while protanopic and deuteranopia luminosity functions can account for atypical eye sensitivity to colors (e.g., color blindness). To first order these alternative luminosity functions are simply shifting the spectral center of the photopic luminosity function.

V. RESULTS

As the primary objective of this test campaign is to assess radiation susceptibility of a variety of COTS pixel technologies, it is pragmatic to jointly evaluate the performance of the emissive displays (LCDs, OLEDs, LEDs). From a human-centric perspective, the most immediate reliability concern for an electronic display would be a decrease in luminosity to the point of functional failure (summarized in Table 2). As a monotone white screen provides the most luminous intensity and would provide the largest contrast ratio for a two-color application (e.g., white text on a black screen). Figure 5 provides luminous intensity values normalized to pre-irradiation values for all emissive displays with a white screen. Degradation in luminous intensity was observed in each electronic display irradiated with a ~10-20% decrease in luminous intensity at 100 krad(Si) for a white screen.

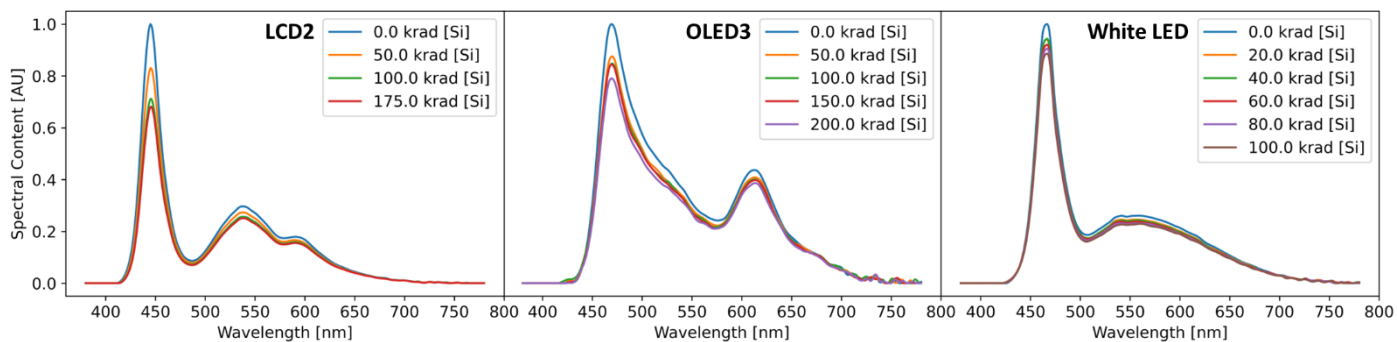


Fig. 6. “White” light spectra as a function of dose for a display from each type of emissive display. The white light spectra of the LCD and OLED are created by a superposition of red, green, and blue pixels spectra with features that can still be seen.

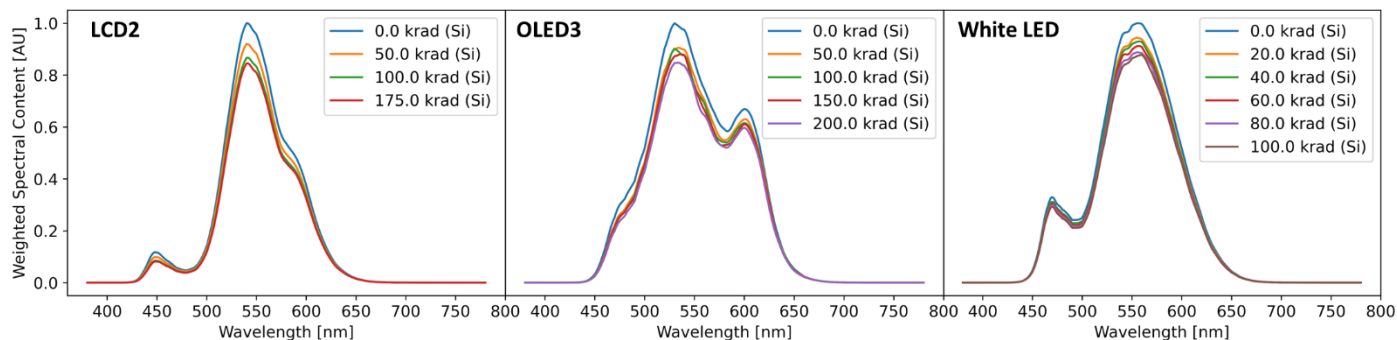


Fig. 7. “White” light spectra weighted with photopic efficiency as a function of dose for a display from each type of emissive display. Note that the degradation in the White LED spectrum across the visible light wavelength range is more uniform than the other emissive displays.

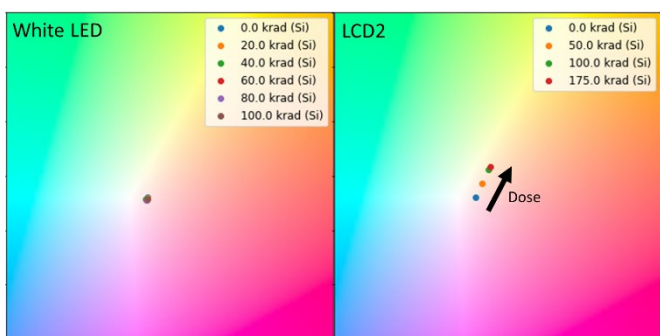


Fig. 8. Color space diagram (CIE 1961) for the “white” light as a function of dose for a white LED and LCD2. Note that the LCD exhibits a shift is away from the blue side of the space towards yellow while the white LED remains a consistent color.

To better understand the degradation observed in the pixels of the electronic displays, it is useful to examine the optical spectra of a display screen configured to display a solid “white” screen as a function of dose. It is notable that the largest degradation in the spectra of the LCD and OLED display screens occurs in the wavelength range associated with the blue pixel compared to degradation in the wavelength ranges corresponding to the red and green pixels. In contrast, the white LEDs exhibit a more uniform degradation across the visible wavelength range (Fig. 6).

The potential for non-uniform degradation of the optical spectra implies that the luminosity intensity of the red, blue, and green pixels will exhibit distinct dose dependence. Using a photopic function as a spectral weight, the impact of radiation-induced degradation on each pixel can be seen on the total luminous intensity of a white screen (Fig. 7). For the white screen of the LCD and OLED display it can be seen that the relative contribution of each pixel to the total luminosity of a white screen degrades at distinct rates and degradation in the

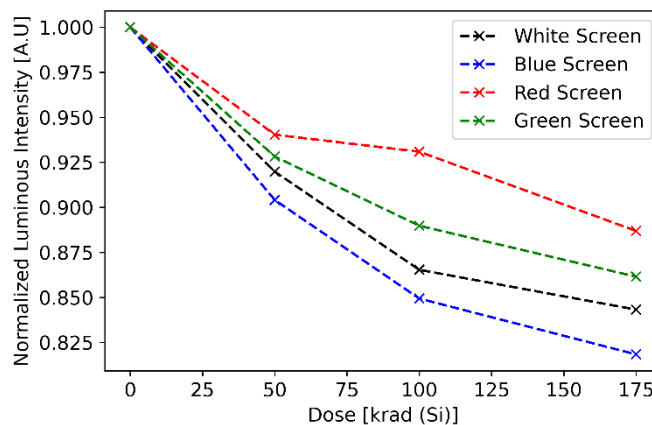


Fig. 9. Luminous intensity normalized to pre-irradiation values for monotone white, blue, red, and green screens for LCD2. Note that the pixel colors degrade at distinct rates.

green pixel dominates the total reduction in luminous intensity of a white screen. The distinct degradation rate of luminous intensity for different color pixels in demonstrated for red, green, blue, and white screens is demonstrated in Fig. 8.

From a human-centric perspective, the results for OLED displays and LCDs imply that the relative contribution of the blue pixel for color mixing decreases as function of dose; this gives the appearance of a white screen developing a yellow hue as dose accumulates while the white LED maintains color purity (Fig. 9). Given that this behavior is observed in both the OLEDs and LCDs despite the differences in functional layers irradiated (e.g., no irradiation of light emission elements in the LCDs or light modulation electronics in the OLEDs) during the test campaign implies that this color shift can be isolated to the additive color mixing process utilized to produce a complete color space. Electronic displays commonly utilize unique contrast offsets and/or gray scale values for each pixel color

meaning that even for a white screen each pixel is being driven with distinct operating conditions. Based on this operating principle it is possible to attribute the degradation to shifting threshold voltages of the TFT-backplane (LCD) and reduction of photon emission from the OLED light emission layer (OLED).

Given the unique behavior of eInk display screens compared to traditional emissive screens, a qualitative approach to accessing radiation-induced degradation was utilized for this test campaign. Rather than actively driving the display with a microcontroller, a persistent test image was uploaded to the display board prior to irradiation and then the command and power pins were grounded to emulate applications utilizing the long-term image retention functionality of eInk display screens. The eInk displays screens were irradiated with 50 krad(Si) dose steps up to a total dose of 200 krad(Si) without presenting any visual degradation of a test image of text on a monochrome background (e.g. no erroneous pixels or perceptible fading). Quantitative measurements analogous to the spectrometer measurements for the emissive displays would likely require additional optical techniques such as spectrographic reflectometry measurements.

VI. TESTING AND MITIGATION CONSIDERATIONS

The observations made from the results of this test campaign can be used to make inferences about testing for radiation susceptibility of candidate electronic displays as well as potential mitigation techniques. In the case of electronic displays that utilize additive color mixing, the potential for distinct degradation rates in the constitutive pixels raises the question of selecting an appropriate test image or understanding the impact of color selection for a mission concept-of-operation. Based on results shown in Fig. 9, using a white light would result capture the largest absolute change in luminous intensity but does not bound the largest relative shift. In addition, utilizing colors that are predominantly based on the red pixel minimizes the relative degradation of luminous intensity of the display.

In regard to mitigation, the most pragmatic technique would be incorporating additional circuitry to dynamically adjust contrast of each pixel color as dose accumulates similar to the existing circuitry incorporated into OLED displays to combat pixel aging. It is worth noting that degradation that modifies the current draw of the displays (e.g., threshold voltage shift in the TFT backplane) can be monitored via power telemetry while degradation mechanisms that strictly impact photon production (e.g., color centers or non-radiative recombination defects) are significantly more challenging to monitor without human intervention. An additional mitigation technique for additive color mixing screens is to consider screens that vary the cross-sectional area or number of each color pixel as way to control operating points of TFT backplanes.

VII. CONCLUSION

A variety of electronic display pixel technologies were considered for radiation susceptibility as next generation crewed missions will necessitate the utilization of electronic displays in a variety of harsh radiation environments. Small-form factor, commercially available electronic displays (LCDs, LEDs, OLEDs, electronic ink/paper) were irradiated using 64 MeV protons to characterize radiation-induced degradation

for human-centric performance metrics such as luminous intensity or color fidelity. Overall, radiation degradation was demonstrated in each of the pixel technologies though the doses and associated degradation are likely to be tolerable for most applications. In addition, the lack of strong TID dose sensitivity suggests that electronic display screens are suitable candidates for system-level single event testing using higher energy protons (e.g., 200 MeV protons commonly found at medical facilities). The lack of significant degradation for an individual pixel technology is notable as it suggests that cumulative radiation susceptibility does not inherently limit the design space of systems with electronic displays.

REFERENCES

- [1] NASA, "Displays and Controls", Apollo Operations Manual, Accessed: Jan. 2023. [Online]. Available: <https://history.nasa.gov/afj/aoh/aoh-v1-3-cont+disp.pdf>
- [2] E. G. Stassinopoulos and J. P. Raymond, "The Space Radiation Environment for Electronics," *Proc. IEEE*, vol. 76, no. 11, pp. 1423–1442, Nov. 1988.
- [3] Landen D. Ryder, Edward J. Wyrwas, and Geraldo A. Cisernos, "Commercial-Off-The-Shelf Small-Form Factor Organic LED and Liquid Crystal Displays Displacement Damage and Total Ionizing Dose Test Report," NASA GSFC, Sept. 2022 [Online] Available: https://radhome.gsfc.nasa.gov/radhome/papers/2022-Ryder-Landen-NASA-TM-22-045_22-046_22-048_22-051-2022Sept28-DD-TID-Test-Report-20230009397.pdf.
- [4] Landen D. Ryder and Edward J. Wyrwas, "SSD1351 OLED Display Driver Single Event Effects Test Report," NASA GSFC, July 2023 [Online] Available <https://radhome.gsfc.nasa.gov/radhome/papers/2022-Ryder-Landen-NASA-TM-22-045-SSD1351-2022Aug-SEE-Test-Report-20230009396.pdf>.
- [5] A. H. Johnston, "Radiation effects in optoelectronic devices", *IEEE Trans. Nucl. Sci.*, vol. 60, no. 3, pp. 2054–2073, May 2013.
- [6] J. R. Srour, C. J. Marshall, and P. W. Marshall, "Review of displacement damage effects in silicon devices", *IEEE Trans. Nucl. Sci.*, vol. 50, no. 3, pp. 653-670, May 2003.
- [7] S. Girard, J. Kuhnenn, A. Gusarov, B. Brichard, M. Uffelen, Y. Ouedane, A. Boukenter, and C. Marcandella, "Radiation effects on silica-based optical fibers: Recent advances and future challenges", *IEEE Trans. Nucl. Sci.*, vol. 50, no. 3, pp. 2015-2036, Feb. 2013.
- [8] Adafruit, "Adafruit 2.4" TFT LCD with Touchscreen Breakout w/MicroSD Socket - ILI9341," Accessed: May 2022. [Online]. Available: <https://www.adafruit.com/product/2478>.
- [9] Adafruit, "3.5" TFT 320x480 + Touchscreen Breakout Board w/MicroSD Socket - HXD8357D," Accessed: Sept. 2022. [Online]. Available: <https://www.adafruit.com/product/2050>.
- [10] Adafruit, "OLED Breakout Board - 16-bit Color 1.5" w/microSD holder," Accessed: May 2022. [Online]. Available: <https://www.adafruit.com/product/1431>.
- [11] Adafruit, "Small 1.2" 8x8 Ultra Bright Blue LED Matrix - KWM-30881CBB," Accessed: Sept. 2022. [Online]. Available: <https://www.adafruit.com/product/1047>.
- [12] Adafruit, "Miniature Ultra-Bright 8x8 White LED Matrix," Accessed: Sept. 2022. [Online]. Available: <https://www.adafruit.com/product/1079>.
- [13] Adafruit, "Adafruit 1.54" Monochrome eInk / ePaper Display with SRAM - 200x200 with SSD1681," Accessed: Sept. 2022. [Online]. Available: <https://www.adafruit.com/product/4196>.
- [14] Adafruit, "Adafruit 1.54" Tri-Color eInk / ePaper 200x200 Display with SRAM - SSD1681 Driver," Accessed: Sept. 2022. [Online]. Available: <https://www.adafruit.com/product/4868>.
- [15] J. F. Ziegler, "SRIM - The Stopping and Range of Ions in Matter," Accessed: Jan. 2023. [Online]. Available: <http://www.srim.org/>
- [16] M.J. Boschini, P.G. Rancoita and M. Tacconi, "SR-NIEL — 7 Calculator: Screened Relativistic (SR) Treatment for Calculating the Displacement Damage and Nuclear Stopping Powers for Electrons, Protons, Light- and Heavy- Ions in Materials (version 9.5)," Accessed May 2023. [Online] Available: <http://www.sr-niel.org/>.

- [17] K. A. LaBel, et al. "A compendium of recent optocoupler radiation test data." *IEEE Radiation Effects Data Workshop*, pp. 123-146, July 2000.
- [18] M. Shaw, M. Fairchild, "Evaluating the 1931 CIE color - matching functions", *Color: Research and Application.*, vol. 27, no. 5, pp. 316-329, Oct. 2002.
- [19] *Multimedia systems and equipment – Colour measurement and management*, IEC 61966-2-1:1999, International Electrotechnical Commission, Geneva, Switzerland, 1999
- [20] K. Sagawa, Y. Takashi, "Spectral luminous efficiency as a function of age", *Journal of the Optical Society of America A*, vol. 18, no. 11, pp. 2659-2667, Oct. 2001